Geoelectric prospecting for water-filled fratured Basement within Kundu, North-central Nigeria

Article · June 2017

CITATIONS
0

READS
43

6 authors, including:

Christopher Unuevho
Federal University of Technology Minna
25 PUBLICATIONS **34** CITATIONS
SEE PROFILE

K.M. Onuoha
University of Nigeria
92 PUBLICATIONS **729** CITATIONS
SEE PROFILE

Amadi Akobundu Nwanosike
Federal University of Technology Minna
173 PUBLICATIONS **1,192** CITATIONS
SEE PROFILE

Emmanuel Emeka Udensi
Federal University of Technology Minna
17 PUBLICATIONS **89** CITATIONS
SEE PROFILE

GEOELECTRICAL PROSPECTING FOR WATER-FILLED FRACTURED BASEMENT WITHIN KUNDU, NORTH CENTRAL NIGERIA

[1*]C.I. Unuevho, [2a]M. Tswako, [3b]K. M. Onuoha, [1c]A. N. Amadi, [4d]E. E. Udensi, [5e]Oshin, O.
1: Department of Geology, Federal University of Technology, Minna
2: Ministry of Water Resources, Minna, Niger State
3: Department of Geology, University of Nigeria, Nsukka
4: Department of Physics, Federal University of Technology, Minna
5: Department of Earth Sciences, Ajayi Crowther University, Oyo
*Email: unuevho@gmail.com, a: tmary2011@gmail.com, b: mosto.onuoha@gmail.com,
c: geoamaa76@gmail.com, d: eeudensi@gmail.com, e: o.oshin@acu.edu.ng

ABSTRACT

Three out of six boreholes failed in Kundu, which is a town located within the North Central Nigerian basement complex. Fractures are commonly water filled within topographic depressions along buried basement surfaces, because the depressions are groundwater convergent zones. Thus drilling for potable water supply will be more successful if the boreholes penetrate such fractures. This study was conducted to delineate fracture bearing topographic depressions in Kundu. It was accomplished by integrated stratigraphic and structural interpretation of geoelectrical data, global digital elevation model (GDEM), and exposed lithological units. Hillshade view of the GDEM for Kundu revealed NW-SE displaced major fractures. The dominant lithological units are gneiss and schist. Electrical resistivity, spontaneous potential and induced polarisation data were acquired by Schlumberger sounding, using ABEM SAS 4000 meter. Two groundwater convergence zones were delineated within two confined fracture intervals. The convergence zone associated with the deep fracture interval exists within the central part of the town. The productive boreholes exist within this zone. Drilling more boreholes within the deep convergence zone will increase access to potable water. The shallow convergence zone is a region for productive borehole drilling around the SW of the town, where none has been sited.

KEYWORDS: *Basement complex, fractures, topographic depressions*

Introduction:

Kundu is a small town within north central Nigerian Basement Complex (figure 1). Groundwater occurrence is localised and difficult to be predicted in basement terrains. This makes locating sites for water borehole drilling very challenging in basement complex areas (Davis & Dewiest 1966). Direct current prospecting has been widely employed in groundwater prospecting in basement areas (Badmus & Olatisu 2012; Ayuk *et al.* 2013; Kumar *et al.* 2014; Ojoina 2014). However, boreholes drilled solely on the basis of resistivity contrast have sometimes failed to produce water. This is probably because similar resistivity anomaly pattern is produced by dry igneous and metamorphic rocks with conductive mineral impregnations (Unuevho *et al.* 2012).

Out of six boreholes drilled in Kundu, only three are productive. The productive three are inadequate to meet domestic demand for water in the town. Dan-Hassan and Olorunfemi (1999), and Olorunfemi (2009) highlighted that boreholes drilled within groundwater convergence zones in Nigerian basement complex are commonly productive, while those drilled within divergence zones are often dry. By virtue of the foregoing, drilling boreholes to penetrate fractures within groundwater convergence zones should increase potable water supply to adequately

meet domestic water needs in Kundu. Consequently, this study was skewed towards delineating groundwater convergence zones from integrated stratigraphic and structural interpretation of electrical resistivity (ER), spontaneous potential (SP) and induced polarisation (IP) data, global digital elevation model (GDEM), and exposed lithological units. Such integrated approach has not been previously employed in prospecting for groundwater in Kundu.

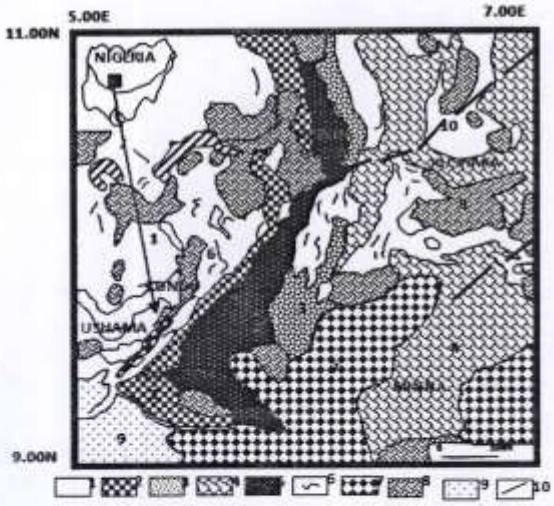

Key:
1. Migmatite gneiss (pre-Pan-African)
2. Kyaniteand silimanite bearing quartzite
3. Zungerumylonite
4. Kushaka Formation
5. BirninGwari Formation
6. Ushama Schist Formation
7. Foliated Tonalite
8. Late Pan-African granite
9. Cretaceous to Recent sediments
10. Major Fracture.

Figure 1: Study Area within Regional Geological setting (Ajibade, *et al.*1989)

Methodology

Advanced Space Borne Thermal Emission and Reflection Radiometer's Global Digital Elevation Model (ASTER's GDEM) for Kundu was obtained from *https://reverb.echo.nasa.gov*. The elevation model was geo-referenced and processed into hillshade view using *ArcMap GIS* software. Lineaments were identified and interpreted to represent fractures. The fractures' displacement directions were identified, and the displacement was associated with faulting. Surface lithological mapping of the town and its environs followed. Subsequently, vertical electrical sounding comprising ER, SP and IP were conducted along ten traverses at an average of five stations per traverse. The traverses were oriented along foliation dip direction (SSE) while measurement electrodes were planted along foliation strike, using Schlumberger electrode geometry. This pattern of data acquisition minimises the influence of lateral lithologic variations that would occur if electrodes are planted in dip direction. The geographical coordinates of the electrical measurement stations were determined using the GPS (Global Positioning System).

Apparent resistivity (ρ_a) was calculated from electrical resistance, R, which the equipment (*ABEM SAS 4000* device) measured directly using:

$$\rho_a = GR \qquad (1)$$

$$G = \frac{\pi}{4}\frac{(AB)^2 - (MN)^2}{MN} \qquad (2)$$

In equation 1 above, G represents geometrical factor related to the electrode geometry, while AB and MN in equation 2 represent current electrode spacing and potential electrode spacing, respectively. Calculated and cumulative ρ_a values were plotted against half electrode spacing (AB/2) on log-log graph sheets. Cumulative ρ_a method of Raghunath (2006) was employed to estimate approximate number of geoelectric layers and depth to their respective top. The values obtained were adjusted using measured thickness of top soil and weathered unit at road cutting and other exposed sections. Each geoelectric layer was assigned an approximate ρ_a .The assigned ρ_a value marks a distinct discontinuity in the pattern of variation in ρ_a values within vertically adjacent geoelectric layers. The approximate number of layers, estimated depth to their respective top, and the approximated ρ_a for each layer, measured ρ_a and AB/2 data were inputted into *WinResist* (indirect resistivity modelling software) to generate geoelectric sections. Each geoelectric section was subdivided into soil, weathered layer, unconfined fractured basement, shallow confined fractured basement and deep confined fractured basement using distinct discontinuity in the pattern of variation in ρ_a values. Respective SP and IP value that is representative of the values within a geoelectric layer were chosen for each layer.

The depth to the top of fresh basement surface underlying each confined fractured basement was subtracted from the corresponding station elevation (obtained using a GPS). This gave the depth of the fresh basement's top with respect to sea level. The depth values were contoured with respect to stations' geographic coordinates (using *surfer*11 contouring software) to generate the fresh basement topography. Depressions within the fresh basement topography were identified. Confined fractured basement ρ_a, thickness, SP and IP values were also contoured. A mosaic map of each confined fractured basement's ρ_a, SP and IP values, as well as elevation of their underlying fresh basement's top (with respect to sea level) was produced. Basement depression areas that are characterised by both low ρ_a and 10-20ms IP values within the mosaic map were interpreted to be groundwater convergence zones that possess groundwater saturation attributes. The location map of the existing boreholes in Kundu was produced, and the positions of the productive boreholes were compared with the groundwater convergence zones (Olorunfemi & Okhue 1992; Dan-Hassan & Olorunfemi 1999; Olorunfemi 2009).

RESULTS

Figure 2 is the hillshade view of the ASTER's GDEM for Kundu and its environs. It revealed major fractures displaced NW-SE by faulting. The geological map produced from surface lithologic mapping is figure 3. It revealed that gneiss; schist, amphibolites and quartzite underlay Kundu and its environs. The gneiss, schist and amphibolite trend NNE, and dip 20 to 60° SSE.

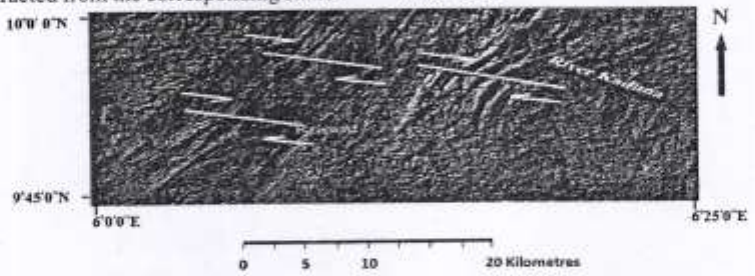

Fig 2: Hillshade topographic image for Kundu and environs

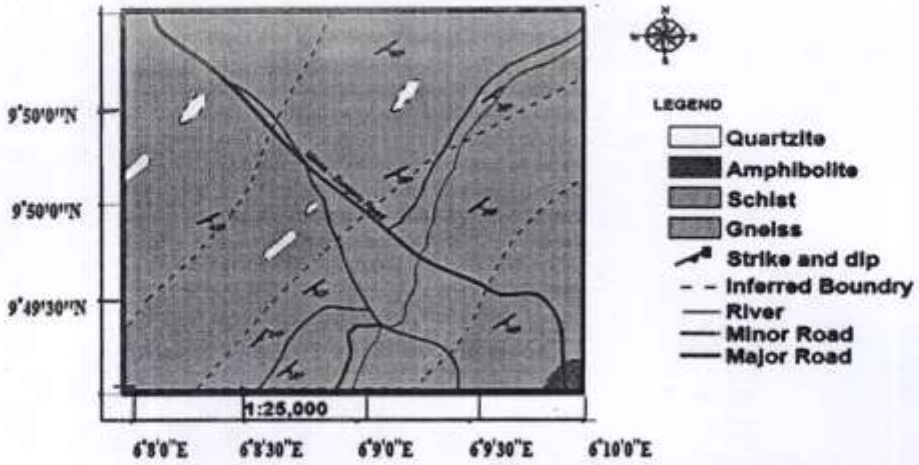

Examples of major surface fractures that indicate polyphase deformation are figures4, 5 and 6. The surface manifestations of polyphase tectonic deformation in Kundu suggest the existence of different confined fractured basement columns in the subsurface.

Figure 4: Unconfined fractures discharging water into River. Kaduna (N9°50'; E6°10')

Figure 5: Fracture imprints of polyphase tectonic deformation in Kundu's neighbourhood N9°49'6.3"; E6°9'7.5"

Figure 6: Unconfined fractures at on schist outcrop at N9°50'; E6°10'

Figure 7 is map of the spatial locations of the sounding stations.

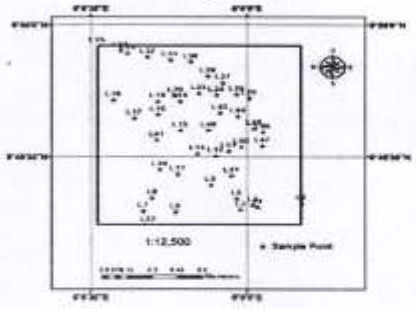

Figure 7: Spatial location of the sounding stations

The apparent resistivity data, modelled resistivity curves and geoelectric layers that are representative of Kundu are presented as figures 8 to 16. The identified curve types and number of geolectric layers are shown in table1. Q- Type curves were not identified. The captured geoelectric layers, which range from 5 to 10 layers, validate the presence of the confined fractures. The layers represent various combinations of H and K curves. The fractures were distinguished into shallow confined fracture and deep confined fractured columns. Drilling monitoring in Minna region of North Central Nigerian Basement Complex sometimes indicates penetration of regolith and shallow (or first)fresh basement units before encountering deep fractured basement aquifer unit at depths over 70m. The shallow confined fracture column is sandwiched between the first fresh basement (unweathered and unfractured basement directly underlying the regolith) and second fresh basement (surface of fresh basement that underlay the shallow confined fractured basement

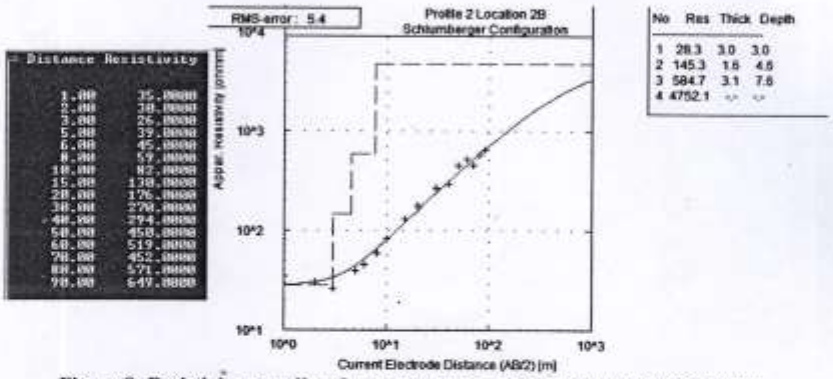

Figure 8: Resistivity sounding data, computer- modelled true resistivity curve geoelectric Layers at VES 5 station

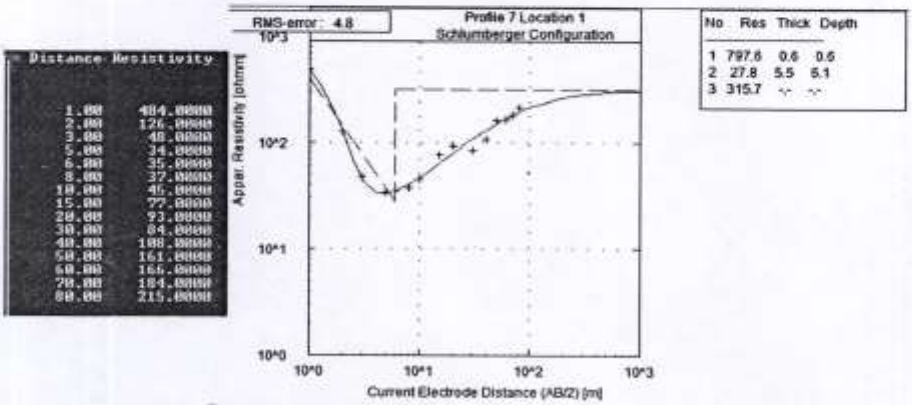

Figure 9: Resistivity sounding data, computer- modelled true resistivity curve and geoelectric Layers at VES 21 station

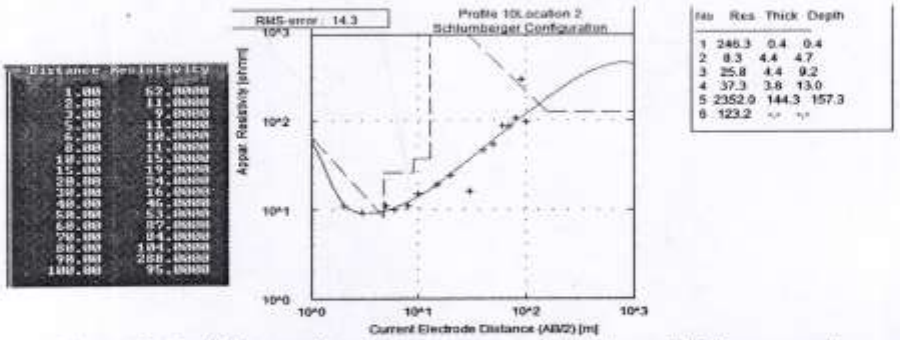

Figure 10: Resistivity sounding data, computer- modelled true resistivity curve and geoelectric Layers at VES 42 station

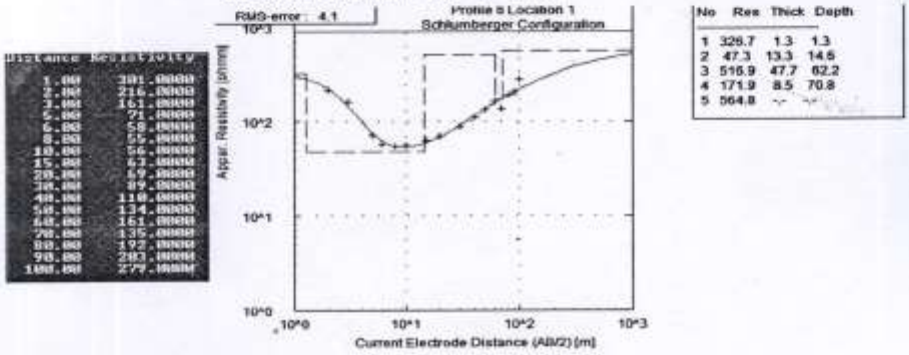

Figure 11: Resistivity sounding data, computer- modelled true resistivity curve and geoelectric Layers at VES 19 station

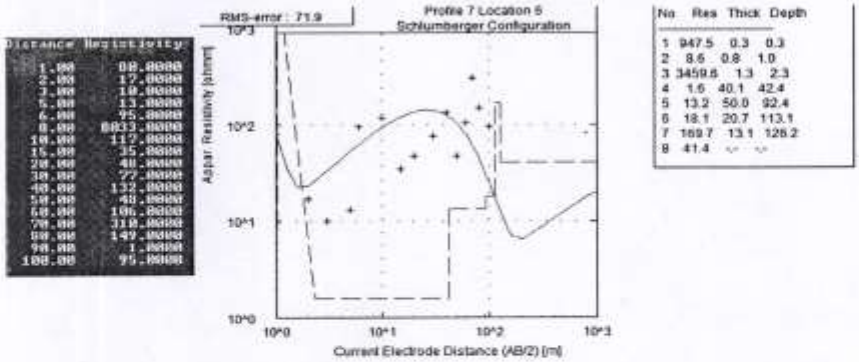

Figure 12: Resistivity sounding data, computer- modelled true resistivity curve and geoelectric Layers at VES 27 station

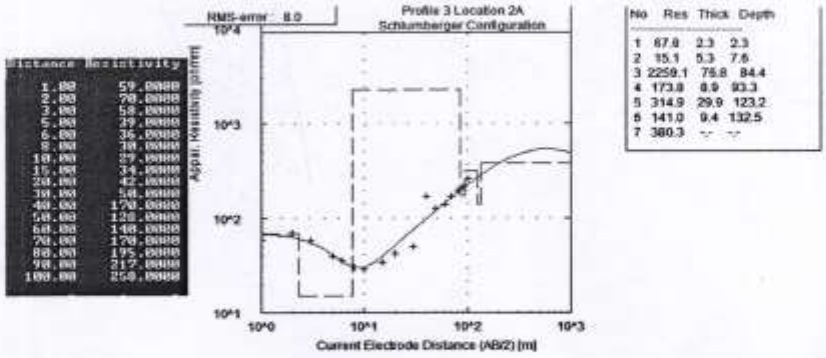

Figure 13: Resistivity sounding data, computer- modelled true resistivity curve and geoelectric Layers at VES 12 station

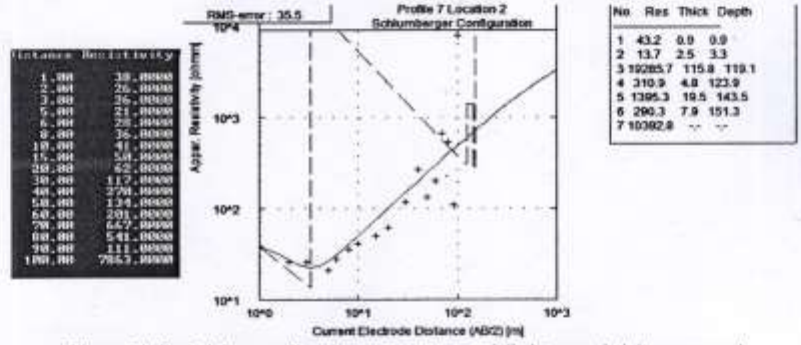

Figure 14: Resistivity sounding data, computer- modelled true resistivity curve and

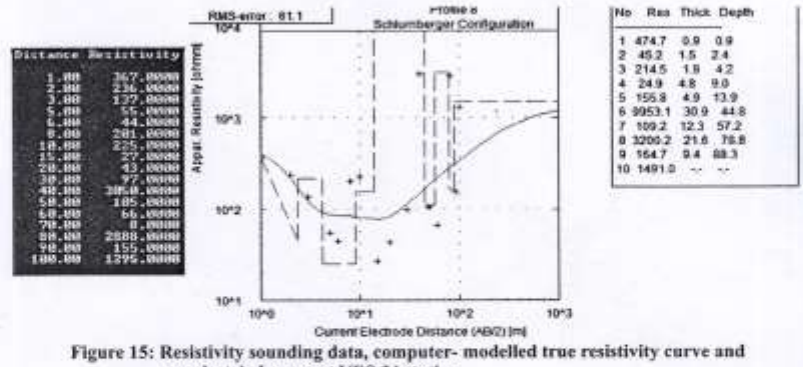

Figure 15: Resistivity sounding data, computer- modelled true resistivity curve and geoelectric Layers at VES 34 station

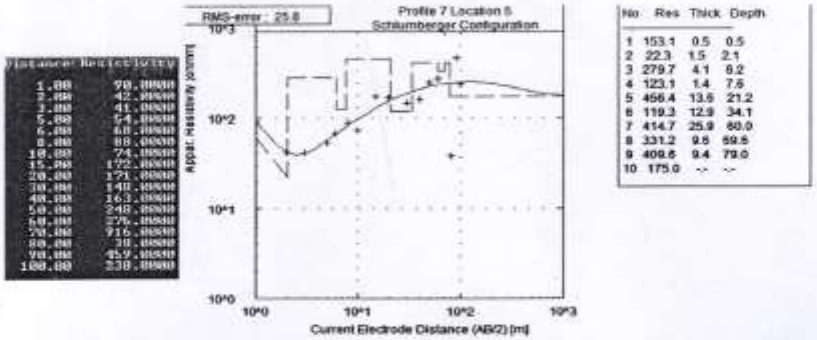

Figure 16: Resistivity sounding data, computer- modelled true resistivity curve and geoelectric Layers at VES 26 station

TABLE 1: CURVE TYPES AND GEOELECTRIC LAYERS WITHIN KUNDU

STATION	CURVE TYPE	GEOELECTRIC LAYERS	STATION	CURVE TYPE	GEOELECTRIC LAYERS
VES 5	A	3	VES 12	HKHKH	7
VES 21	H	3	VES 23	HKHKHK	8
VES 42	HK	4	VES 34	KHKHKHK	9
VES 19	HKH	5	VES 26	HKHKHKHK	10
VES 27	HKHAK	7			

Tables 2 and 3 are SP and IP values measured at sounding stations with VES data that are representative values for Kundu. Figures 17, 18, and 19 are respectively the thickness map, resistivity map and induced polarisation effect map for the shallow confined fracture column. The thickness of this fractured column ranges from 2 to 40m. The resistivity of the column ranges from 300 to 11500?m.

Table 2: Spontaneous potential values obtained at VES stations 5, 9,12, 15, 21, 23, 26, 34

AB/2	SP 5 (mv)	SP 9 (mv)	SP 12 (mv)	SP 15 (mv)	SP 21 (mv)	SP 23 (mv)	SP 26 (mv)	SP 34 (mv)
1	35.77	75.46	86.1	9.17	0.113	-0.108	-70.99	49.59
2	36.85	75.1	-79.65	10.32	0.113	- 0.11	-71.53	51.94
3	36.95	72.53	-71.85	11.01	0.107	-0.111	- 69.6	53.5
5	37.21	65.97	-68.64	11.43	0.102	-0.114	-9.515	57.98
6	65.42	81.995	-73.275	19.49	86.045	-1.643	6.95	35.4835
8	91.84	-70.17	53.27	- 1.07	98.71	-3.198	16.14	9 .695
10	74.21	-29.365	51.565	30.94	83.69	-2.242	18.1905	29.34
15	41.79	-98.06	- 78.3	54.55	77.55	0.536	55.67	-51.84

AB/2	SP 5 (mv)	SP 9 (mv)	SP 12 (mv)	SP 15 (mv)	SP 21 (mv)	SP 23 (mv)	SP 26 (mv)	SP 34 (mv)
20	39.57	-69.86	- 86.7	56.14	88.12	2.937	52.67	-54.32
30	39.91	-53.42	-92.34	57	90.61	8.97	57.78	1.101
40	37.11	19.9965	42.6205	28.5035	66.27	65.16	65.54	25.402
50	57.97	0.113	0.138	0.149	32.78	39.28	34.05	0.103
60	66.25	93.05	0.15	0.138	41	40.57	40.76	0.104
70	66.38	77.85	0.159	0.126	44.21	43.83	50.49	0.104
80	33.21	33.435	0.5455	33.068	42.79	22.95	0.801	- 0.78
90	0.247	78.51	-80.09	46.62		0.155	0.343	- 0.25
100		27.339	-40.74	46.31		27.264	30.614	-14.09

Table 3: Induced polarisation values obtained at stations IP5, 9, 12, 15, 21, 23, 26, 34

AB/2	IP 5 (ms)	IP 9 (ms)	IP 12 (ms)	IP 15 (ms)	IP 21 (ms)	IP 23 (ms)	IP 26 (ms)	IP 34 (ms)
1	1.51	0.47	0.64	1.12	1.37	2.45	0.33	0.33
2	1.05	0.79	0.83	0.14	1.91	-1.24	2.59	2.59
3	-3.09	1.4	-2.65	0.58	2.18	1.92	151	151
5	-3.91	0.5	-1.4	-1.9	2.82	-4.68	63.1	63.1
6	-10.735	0.485	0.67	2.395	2.46	83.145	-507	-507
8	-4.74	-0.68	0.63	7.93	1.85	30.7	-378	-378
10	5.84	0.69	1.345	1.463	1.635	73.05	42.5	42.5
15	-0.053	1.25	0.81	1.65	0.96	0.78	-30	-30
20	-3.43	0.069	1.75	-0.057	0.41	0.75	-5.77	-5.77
30	-3.61	0.056	0.26	-1.48	4.14	10.3	-78.3	-78.3
40	-19.815	0.795	1.255	-3.77	2.79	-609	-98.9	-98.9
50	-1.78	0.78	0.73	-1.57	1.36	-4.67	227	227
60	-2.1	0.51	0.45	-2.26	2.3	13.7	17.9	17.9
70	-17.5	0.57	-0.93	-1.36	2.42	-275	-124	-124
80	11.75	0.985	0.545	3.06	2.225	-422.45	-278.5	-278.5
90	-7.65	0.17	-1.37	0.4		-7.58	-147	-147
100		0.3	0.29	6.285		2.84	297.5	297.5

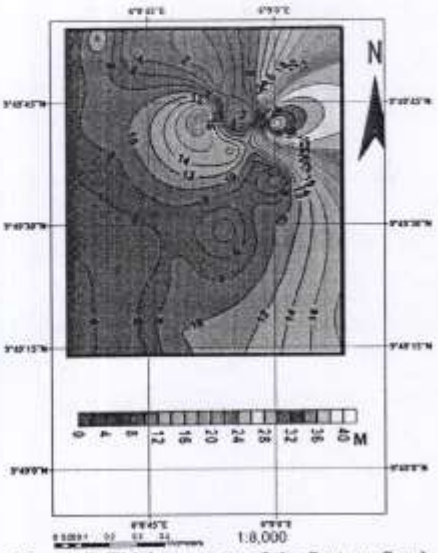

Figure 17: Thickness map of the first confined fractured basement column

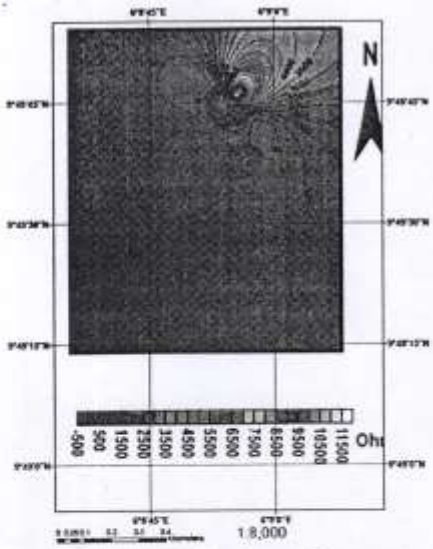

Figure 18: Resistivity fractured basement column map of the first confined

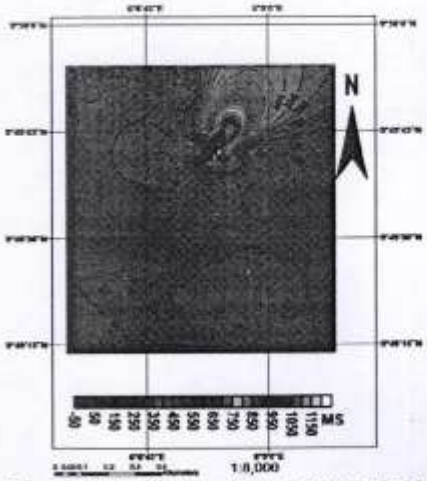

Figure 19: IP effect map for the first confined fractured bedrock in Kundu

Figure 20 is the elevation map (with respect to sea level) of the second fresh basement surface, which is the fresh basement surface that underlies the shallow fractured column. The elevation map reveals a topographic depression on its south western portion. This topographic depression is probably a ground water convergence zone within the first confined fractured basement column. The SP map for the shallow confined fractured basement is presented as figure 21.

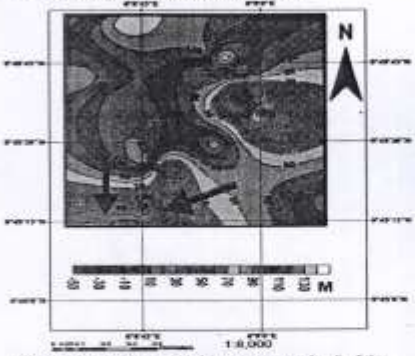

Figure 20: Elevation map (with respect to sea level) of the second fresh basement surface (surface of fresh basement that underlain the first confined fractured basement column)

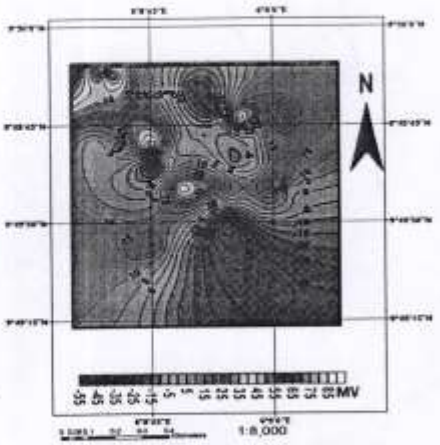

Figure 21: Map of SP values of the first confined fractured basement column

The deep confined fractured basement column is sandwiched between the second fresh basement interval and third fresh basement. Fig 22, 23, and 24 are respectively the thickness map, resistivity map and induced polarisation effect map for the second confined fracture column. The second confined fracture basement column is thickest in the north western portion, where it is 15 to 25m thick. It is 9 to 14m thick in its central portion and thinnest in its eastern part, where it is 2-7m thick (Fig.22). The column's IP effect values range from 0 to 60ms in the central part (Fig.24).

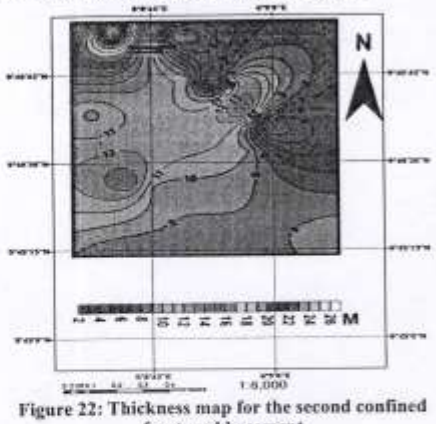

Figure 22: Thickness map for the second confined fractured basement

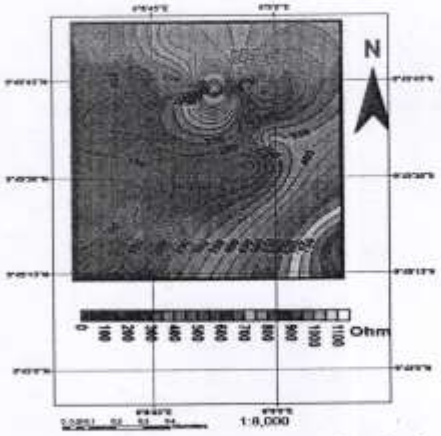

Figure 23: Resistivity map for the second confined fractured basement in Kundu

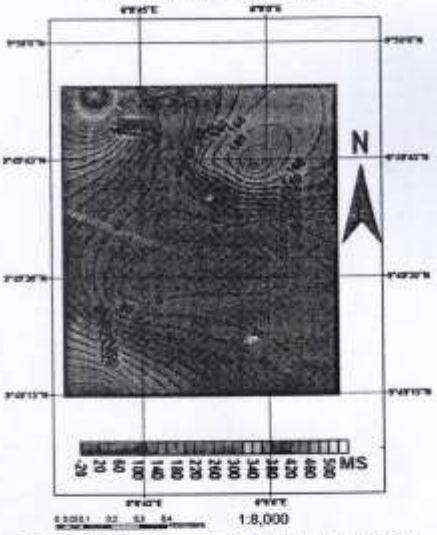

Figure 24: IP effect map for the second confined fractured basement

Discussion

Figure 25 is the mosaic map that captures area within Kundu where basal surface elevation for shallow confined column is lower than 80m(with respect to sea level), and the column's resistivity, IP and SP values are

respectively lesser than 500?m, 50ms and +1mv. It reveals the south western part of Kundu where groundwater convergence zone contains water filled fractures. This is defined by Latitudes N9°49?15?? to N9°49?27?? and Longitudes E6°8'37" to E6°8'45".

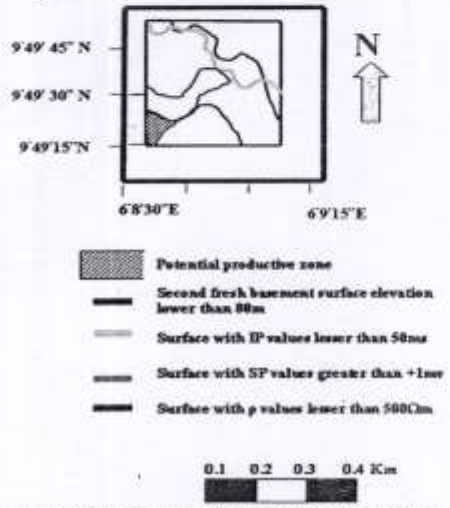

Figure 22: The mosaic map of IP, SP and resistivity values of first (or shallow) confined fractured basement column and elevation of the column's base (the second fresh basement top surface)

The resistivity of the deep fracture column is generally lesser than 300?m, except in the north central portion where it is up to 1000 ?m (Fig.23). This implies that the column is generally characterised by optimal resistivity value that is commonly associated with groundwater occurrence. The column's IP effect values range from 0 to 60ms in the central part (Fig.25). The characterisation of this portion with 0-60ms IP effect and resistivity values of 150 -300 ?m indicate presence water filled fractures in the central part of Kundu.

Figures 26 and 27 are respectively the elevation map (with respect to sea level) for the base of the deep fractured basement column (which is also top surface of the third fresh basement) and SP values map of the second fractured basement column. The deep fracture column occupies a topographic depression in this central part, and thus constitute groundwater convergence zone (Fig.26). The fracture column is associated with +5 to +45mv SP values in this central part (Fig.27). This supports the existence of a topographic depression in the central part of the town.

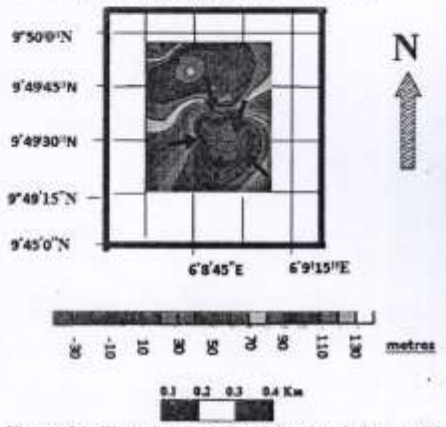

Figure 26: Elevation map for the base of the second confined fractured

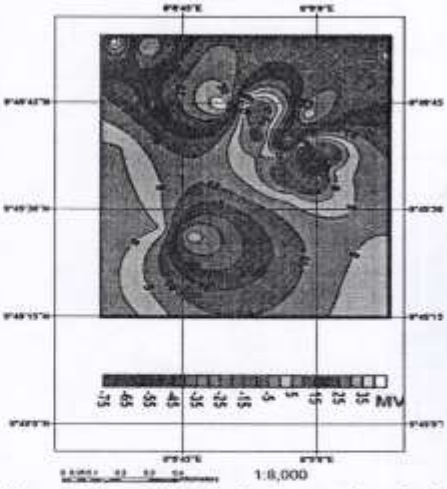

Figure 27: Map of SP values for the second confined fractured basement

Figure 28 is a mosaic map that represents areas where the deep fractured column has ρ_a lower than 300?m, IP values lower than 20ms, SP values higher than +10mv, and basal surface elevation lower than 90m. The basal surface is the fresh basement surface that directly underlies the fractured column. The shaded part of Fig.28 captures the central part of Kundu where groundwater convergence zone contains fractures with water bearing attributes.

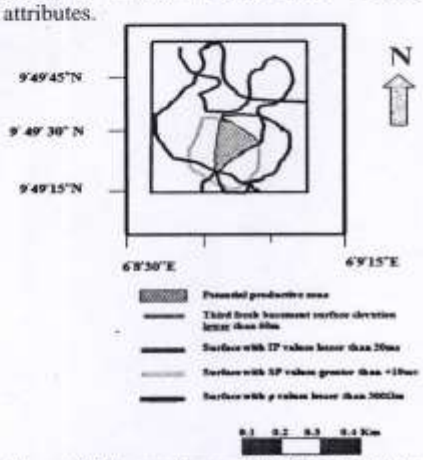

Figure 28: The mosaic map of IP, SP and resistivity values of first (or shallow) confined fractured basement column and elevation of the column's base (the second fresh basement top surface)

Figure 29 is the map showing the locations of the existing boreholes in Kundu. It reveals that no borehole has yet been drilled in this part of the town. Thus the convergence zone in south south- west (SSW) of Kundu constitutes a drilling prospect. The productive boreholes (W1, W2 and W6) are located within the shaded portion (Fig.29), where there is high potential for accumulation of producible water. The failed wells (W4, W3) are located on high topographic areas of the elevation map for the base of the deep confined fracture column (Fig.26). Their location on Fig.26 is defined by Latitudes N9°49'44.4" to N9°49'58.8" and Longitudes E 6°8'34.8" to E 6°8'56.4". Another failed well (W5) lies outside the convergence zone. Its location coordinates are Latitude N 9°49'28.4" and Longitude E 6°8'45.6??(figures 26,28 and 29). Thus topographic high zone should be avoided when drilling to tap water from the second confined aquifer. Wells should be drilled within the groundwater convergence zone in this aquifer.

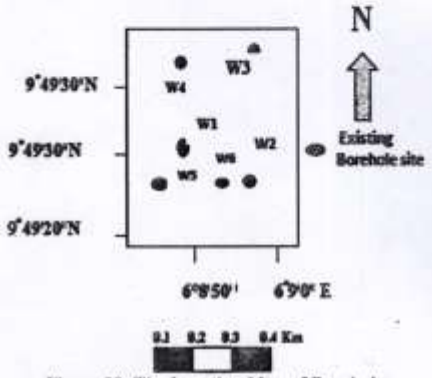

Figure 29: The Location Map of Boreholes

Conclusions

The of H- with K-type curves are geoelectrical imprints of polyphase tectonic deformation driven by multiple orogenic regimes experienced in kundu and its neighbourhood. Integrated stratigraphic and structural interpretation of ER, SP and IP data has revealed confined shallow and deep fractured basement aquifers within groundwater convergence zones in Kundu. The groundwater convergence zone with shallow aquifer exists in the SW (defined within N9°49'15" to N9°49'25" and E 6°8'30" to E 6°8'40") part of the town. It constitutes a drilling prospect since no borehole has yet been drilled to test its groundwater potential. The groundwater convergence zone with deep fractured basement aquifer is located in the central part of the town. The productive boreholes in the town exist within this convergence zone. The failed ones were

drilled in the topographic high zones outside the convergence zone.

Referencess

Ajibade, A.C., Woakes, M. and Rahaman, M.A. 1989. Proterozoic Crustal Development in the Pan African Regime of Nigeria. In :Kogbe, C.A. (Ed.) , Geology of Nigeria. Rock View Nig. Ltd., Lagos.

Ayuk, M.A., Adelusi, A.O., and Adiat, K.A.W. 2013. Evaluation of groundwater potential and aquifer protective capacity assessment at Tutugbua-Olugboyega area, off Ondo road, Akure, SW Nigeria. *International journal of physical sciences*, 8(1): 37-50.

Badmus,B.S. and Olatisu,O.B. 2012. Geophysical characterisation of basement rocks and groundwater potentials using relectrical sounding data from Odeda quarry site, South –Western Nigeria. *Asian journal of earth sciences*, 5(3):79-87.

Dan-Hassan, M.A. and Olorunfemi, M.O. 1999. Hydrogeophysical investigation of a basement terrain in the North Central part of Kaduna State, Nigeria. *Journal of mining and geology*, 36(2):189-206.

Davis, S.W. and De Weist, R.J.M. 1966. *Hydrogeology*. New York: John Wiley and Sons. from resistivity sounding data in parts of Kalmeshwartaluk of Nagpur district, India. *Current science*, 107(7): 1137-1145.

Ojoina, O.A. 2014. Hydrogeophysical investigation for groundwater in Lokoja metropolis, Kogi State. *Journal of geography and geology*, 6, 1(20): 81-95.

Olorunfemi, M.O., 2009. *Groundwater exploration, borehole site selection and optimum drill depth in basement complex terrain*: Water resources special publication series.

Olorunfemi, M.O. and Okhue, E.T. 1992. Hydrogeologic and geologic significance of a geolectric survey at Ile-Ife, Nigeria. *Journal of Mining and Geology*, 28:2

Raghunath, H.M.2006. *Groundwater*, 3rd ed. New Delhi; New Age.

Unuevho, C., Onuoha, K.M. and A lkali Y.B., 2012. Direct current resistivity methods for groundwater prospecting in hardrock terrains: a viable approach to providing sustainable potable water. *Centre for Human Settlements and Urban Development Journal*:1-16.